Directed-Sorting Method for Synthesis of Bead-Based Combinatorial Libraries of Heterogeneous Catalysts

Ramanathan Ramnarayanan, Benny C. Chan, Michael A. Salvitti, and Thomas E. Mallouk*

Department of Chemistry, The Pennsylvania State University, University Park, Pennsylvania 16802

Falaah M. Falih, Jason Davis, Douglas B. Galloway, Simon R. Bare, and Richard R. Willis*

UOP LLC, 25 East Algonquin Road, Des Plaines, Illinois 60017

Received October 9, 2005

The synthesis and analysis of inorganic material combinatorial libraries by a directed-sorting, split−pool bead method was demonstrated. Directed-sorting, split−pool, metal-loaded libraries were synthesized by adsorbing metal salts (H_2PtCl_6, $SnCl_2$, $CuCl_2$, and $NiCl_2$) and metal standards (Pt, Cu, Ni in HCl) onto 2-mg porous γ-alumina beads in 96- or 384-well plates. A matrix algorithm for the synthesis of bead libraries treated each bead as a member of a row or column of a given matrix. Computer simulations and manual tracking of the sorting process were used to assess library diversity. The bead compositions were analyzed by energy-dispersive X-ray spectroscopy, X-ray fluorescence spectroscopy, electron probe microanalysis, inductively coupled plasma atomic emission spectroscopy, and inductively coupled plasma mass spectroscopy. The metal-loaded beads were analyzed by laser-activated membrane introduction mass spectroscopy (LAMIMS) for catalytic activity using methylcyclohexane dehydrogenation to toluene as a probe reaction. The catalytic activity of individual beads that showed minimal (∼20% of that of Pt on alumina) to high conversion could be determined semiquantitatively by LAMIMS. This method, therefore, provides an alternative to screening using microreactors for reactors that employ catalysts in the form of beads. The directed-sorting method offers the potential for synthesis of focused libraries of inorganic materials through relatively simple benchtop split−pool chemistry.

Introduction

We describe here a split−pool, directed-sorting approach for the synthesis of inorganic bead libraries. This work builds on an earlier paper[1] that demonstrated the use of the split−pool concept in solid-state materials chemistry. The biggest challenges in our earlier work[1] were to develop a tagging scheme to track metal salt adsorption and to avoid the mixing of components and dissolution of the alumina support in sequential adsorption steps. These problems resulted in relatively poor control over bead composition as well as an inability to identify individual beads without postsynthesis analysis. The directed-sorting approach demonstrated in this paper, based on matrix methods and adsorption in well plates, enables the synthesis of combinatorial bead libraries without problems of component mixing. The method eliminates the need for postsynthesis bead identification and also eliminates the tagging problem. The sorting algorithm allows one to make compositionally diverse libraries using inexpensive equipment (well plates, plastic pipets) in a relatively small number of steps. To demonstrate this approach, we chose noble metals and 2-mg, porous γ-alumina beads of the kind typically used in heterogeneous catalysis.[2] One library was evaluated for catalytic activity by laser-activated membrane introduction mass spectrometry (LAMIMS).[3] We chose methylcyclohexane (MCH) dehydrogenation to toluene as a probe reaction.

The split−pool method allows one to synthesize a bead library by choosing *n* components, which in the case described here are adsorbed onto the beads in *n* well-plates and *m* split−pool steps. The individual beads are sorted by using a predetermined algorithm that tracks the history of each bead as metal salts are adsorbed onto it. These sorting algorithms simplify the mapping of a multidimensional composition space into a 2-D array layout. By changing some of the parameters of the sorting algorithm, such as the sequence of row- and column-shuffling steps, it is possible to change the compositional redundancy of the resulting split−pool library. This control is enabled by replacing the vials described in ref 1 by wells in standard commercial well plates. This simple modification, illustrated in Figure 1, solves the component mixing problem by isolating each bead in a unique well, physically separated from the adjacent beads. Each bead absorbs the same amount of solution in each step. The tagging problem is solved by indexing every bead by four coordinates (well plate identity, row and column number, and split pool step). The most important outcome is the direct correlation of the response of the library (to a probe reaction or signal) with the composition and sequence of metal adsorption steps on each bead without physical tagging.

10.1021/cc050137r CCC: $33.50
Published on Web 01/20/2006

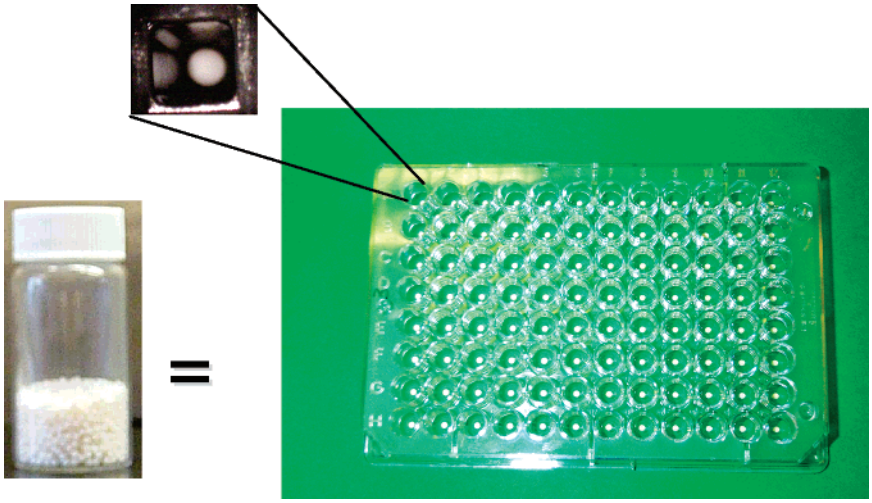

Figure 1. Schematic illustrating the advantage of replacing beads in vials by beads in well plates to solve the mixing and tagging problems. The wells in each plate are indexed by their rows and columns, and each plate is indexed by a unique identifier that corresponds to one chemical component of the bead library.

The concept of spatially addressing a large number of experiments can be traced to the work of Mittasch,[4] who tested large numbers of catalysts and, in essence, kept track of every sample and its processing history. Computers were not invented in 1903, and one can assume that laboratory notebooks and entries therein served as tags. To our knowledge, the earliest documented systematic way of designing experiments following a specific algorithm can be traced to the work by Fisher and Yates,[5] who were interested in problems in biology and agriculture, leading to useful concepts such as analysis of variance (ANOVA) and design of experiments (DOE). With the advent of combinatorial methods pioneered by Hanak[6] and popularized by numerous researchers,[7−15] sophistication increased along with the use of computers and robotics. Labor-saving DOE constructs were generally not used in this early work, because they were not easily integrated into the array deposition methods used.[16] The method described here utilizes computer simulations of the directed-sorting process to gauge the diversity and redundancy of the resulting bead libraries; in principle, screening data from such libraries are amenable to analysis by ANOVA and related statistical methods.

Split−pool combinatorial approaches have been widely used in organic and bioorganic chemistry and have been extensively reviewed.[2,16,17] Directed-sorting approaches to making split−pool materials libraries were reported by our group and by Schunk et al.[1,15] Schunk et al.[15] describe the synthesis and characterization of a 3000-member Mo−Bi−Co−Ni−Fe-on-γ-alumina library. Their synthetic procedure for adsorption involved adsorbing metal salts onto γ-alumina in a porcelain dish, which was similar to the adsorption in vials described in our earlier work.[1] Post analysis of beads was still required in their method to identify bead compositions.

Experimental Section

Materials. H_2PtCl_6, $SnCl_2 \cdot 2H_2O$, $CuCl_2 \cdot 2H_2O$, and $NiCl_2 \cdot 6H_2O$ were purchased from Alfa Aesar and used as received. Pt, Co, Cu, and Ni analysis standards (1.0 mg and 10 mg in 1.00 mL of 2.00 and 10.0% HCl) were purchased from Hi-Purity Standards and used as received. Porous γ-alumina beads made by an oil drop technique[18] had a surface area of 195 m^2/g and an average diameter of 1.5 mm. The average mass of the support beads was 2.3 mg. Prior to first adsorption, γ-alumina beads were washed in DI water at room temperature. The beads were then calcined at 400 °C for 3 h to remove excess water and allowed to cool to ambient temperature. Vaccu-pette 96 (a plastic device for transferring solutions to standard 96-well plates), well plates, and pipets were purchased from VWR. Cascade Blue, Fluorescein-5-isothiocyanate, Lucifer Yellow, and Sulforhodamine 101 were used as received from Molecular Probes.

One Sphere at a Time (OSAAT) Experiments Under Incipient Wetness Conditions. In OSAAT experiments, one alumina sphere was placed manually into each well of a 96 V-bottom well plate (Nalge Nunc International). To reduce the effects of variable diameter and weight of the beads during these experiments, we manually sorted about 700 beads by weight (2.3 ± 0.2 mg) and diameter (sieved using a 1536-well plate). The beads were then divided into six equal lots (~100 beads each). Metal salts were dissolved in 0.5 M HCl to a final concentration of 0.09 g/mL. In a typical procedure to adsorb 0.05 wt % Pt onto each bead, ~1.8 g of H_2PtCl_6 (Alfa Aesar) and 530 μL of concentrated hydrochloric acid were dissolved in 20 mL of water. The solutions were heated to boiling for 15 min, cooled to room temperature, and then diluted to 25 mL. During the adsorption experiments, 12 μL of solution containing the metal salt was manually delivered at room temperature and by means of a pipet to each well containing a bead. The beads were then dried at 60 °C for 1 h in the well plates. Adsorption under these conditions is close to incipient wetness. We also examined the adsorption of Ru, Ni, Au, Pd, Re, Ir, and Rh using the following metals salts dissolved in 0.5 M HCl: H_2PtCl_6, $RuCl_3$, $RhCl_3$, $Pd(NO_3)_2$, $HAuCl_4$, $NiCl_2$, H_2IrCl_6, and NH_4ReO_4 (Alfa Aesar).

Modifying the Vaccu-pette for Bead Transfer and Use as a Multipipet. In combinatorial chemistry experiments to date and in OSAAT experiments described in our earlier paper (see refs 1, 2 and references therein), robotic plotters

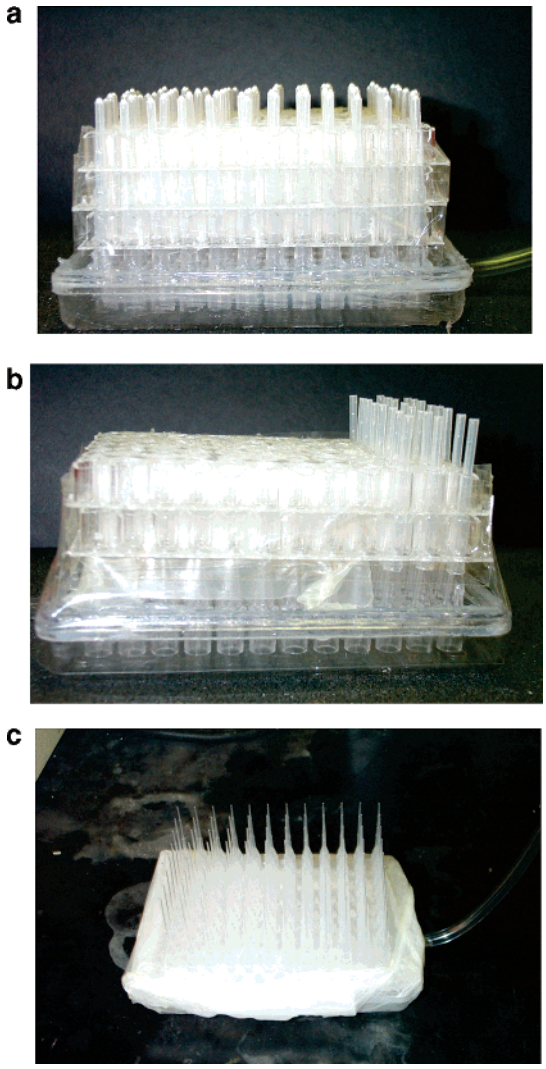

Figure 2. Home-built vacuum pipetting devices for (a) transferring beads across rows and columns, (b) sorting along rows, and (c) delivering solutions of 0−20 μL.

or printers have typically been programmed to deliver the metal salt solutions needed to synthesize large libraries. Here, a Vaccu-pette, which is an inexpensive plastic multitip pipettor, was modified to make a multipipet syringe and bead transfer device. To use the Vaccu-pette as a bead transfer device, Samco Transfer pipet tips were cut to 4.4-cm length and attached to the Vaccu-pette bottom using a 96-well plate. Holes were drilled into the wells of a 96-well plate, and the pipet tips were held onto the Vaccu-pette using the hollow plate and cellophane tape, as shown in Figure 2a and b. To use the Vaccu-pette as a multipipettor, paraffin wax was melted in a crystallization dish. Pipet tips used to deliver solution (0−20 μL) were held onto the pegs of the Vaccu-pette, and the whole assembly was immersed in hot paraffin wax. The wax was cooled to room temperature, and the assembly was removed from the wax using a heated chisel. The bottom of the multipipettor was encased in Parafilm as shown in Figure 2c. This simple set of tools eliminates the need for expensive synthetic equipment, such as commercial plotters and solid handling devices often used in combinatorial chemistry.

Elemental Analysis. Metal loadings and distribution on representative beads were determined by using energy-dispersive X-ray spectroscopy (EDS), micro X-ray fluorescence (μ-XRF), and inductively coupled plasma atomic emission spectrometry (ICP-AES) at UOP and electron probe microanalysis (EPMA) and inductively coupled plasma mass spectrometry (ICP-MS) at Penn State. ICP-AES analysis was performed on a Leeman Labs PS3000 using calibration standards (Specpure from Alfa Aesar and Hi-Purity Standards). ICP-MS analysis was performed using a Finnigan MATELEMENT high-resolution instrument using the same calibration standards as in ICP-AES. For ICP-MS analysis, the beads were digested for 1 h at 80 °C in a mixture of 2 mL of DI water, 2 mL of concentrated H_3PO_4 (EMD from VWR), and 1 mL of concentrated HCl (EMD from VWR) in Erlenmeyer flasks covered with a watch glass; cooled to room temperature; and diluted to 50 mL with DI water. Calibration standards containing Cu, Co, and Ni were also diluted to 50 mL in the same matrix as the samples. Indium (10 ppb) was used as an internal standard in all samples used for ICP-MS, and data were normalized to In counts in the mass spectrometer. For some of the samples that had errors >20% by ICP-MS, Cu and Ni calibration standards (Hi-Purity) were spiked together with In, and samples were reanalyzed. EPMA analysis used a Cameca SX-50 by sectioning each bead into two halves and mounting in epoxy. EPMA profiles were recorded from the edge to the center in 50-μm steps with a 20-μm spot size; because of epoxy penetration, data were not acquired within 20 μm of the bead edge. EDS spectra from the bead edge for the beads adsorbed with Pt were collected on a scanning electron microscope (JEOL 840), which was operated at 15 kV and a beam current of 600 nA, with counting time of 200 s and spot size of 10 μm^2. The elemental concentrations were extracted by a linear least-squares fit to spectra of standards recorded in the same instrument under the same conditions. Peak deconvolution, integration, and conversion to wt % were performed using Noran software. The EDS elemental maps for the beads adsorbed with Pt, Ru, Ni, Au, Pd, Re, Ir, and Rh were collected on a scanning electron microscope (JEOL JSM 5400) with the IMIX-PC version 10.593. The spectra were recorded at a takeoff angle of 30°, accelerating voltage of 20 KV at a magnification of 75×. Each EDS elemental map was collected for 1 h. Under these conditions, the detection limits of the EDS system were reached at 0.3 wt %. We therefore concluded that the EDS system was able to detect metal at loadings on the beads of 0.5 wt % or more. Samples were also analyzed by micro-XRF (Eagle III μProbe from EDAX) using a Rh−Kα source at an excitation energy of 25 keV. The spot size was 1 mm, and the collection time used was 300 s/bead. On the basis of the beam excitation energy, the escape depth was estimated to correspond to the outer 200 μm of the γ-alumina bead.

Directed-Sorting Experiments. The first step in the split−pool synthesis process was adsorption. This was done by transferring beads using the modified Vaccu-pette shown in Figure 2a. Once metal salt solutions were adsorbed onto the beads and dried, rows of beads from a given plate were transferred using the row-sorter shown in Figure 2b to a set of receiving well plates. The process was repeated cyclically. For example, in a four-component split−pool synthesis,

Table 1. ICP-AES of Pt on γ-Alumina

	sample no.				
theor wt %	1	2	3	av wt %, exptl	SD
0.05	0.048	0.052	0.054	0.051	0.003
0.1	0.11	0.103	0.104	0.106	0.004
0.15	0.162	0.149	0.146	0.152	0.009
0.2	0.181	0.196	0.178	0.185	0.01
0.5	0.444	0.442	0.482	0.456	0.023
1	0.953	1.02	0.986	0.986	0.034

which involves four receiving well plates, one-fourth of the rows are transferred in rows to the first well plate, one-fourth to the next, and so on. This process happens four times per plate for a four-component row shuffle, as illustrated in Figure 3a. The same procedure was used for the column shuffle, with the transfer being perpendicular to that described above. The row- and column-shuffle steps alternated, with a row shuffle after every odd adsorption step (counting the first as odd) and a column shuffle after every even adsorption step, as shown in Figure 3b,c. These steps are repeated for *m* sorting steps, making the total number of adsorptions *m* + 1. In the sorting algorithm represented by Figure 3 and Tables 2 and 3, a shift by one row and one column was added after every pair of row/column directed-sorting steps to maximize the diversity of the bead libraries. For example, in the synthesis of a four-component bead library occupying four 96-well plates (12 rows × 8 columns), rows of beads were moved in groups of three and columns in groups of two. In the first row shuffle, rows 1−3 from plate 1 were transferred to plate 1, rows 4−6 to plate 2, etc. In the second row shuffle, rows 12, 1, and 2 from plate 1 were transferred to plate 1, rows 3−5 to plate 2, etc., as illustrated in Figure 3c. In the third row sort, rows 11, 12, and 1 from plate 1 were transferred to plate 1, rows 2−4 to plate 2, etc. The adsorption and sorting operations were alternated until the desired number of split−pool steps was achieved. The directed-sorting procedure, thus, replaces vials described in ref 1 by well plates.

Test for Methylcyclohexane Dehydrogenation to Toluene Using LAMIMS. The design of the LAMIMS system used for comparing the activities of catalyst beads has been described previously by Nayar et al.[3] Hydrogen gas was passed through the reactor at 50 mL/min, and a 25-W laser (Synrad) was held over each bead for 6 min at 25% laser power to reduce metal salts to metal at each bead. The laser wavelength was 10.57−10.63 μm, and the spot diameter was 3.5 mm. The feed was switched to a mixture of H_2 (50 mL/min) and MCH (0.02 mL/min). The laser was switched to 55% peak power and held at each bead for 40 s to provide energy to heat the bead and the gas surrounding the bead and to provide energy needed for the endothermic reaction (MCH to toluene) and for toluene to desorb. Laser energy estimates for bead reduction and LAMIMS analysis are given in the Supporting Information.

Results and Discussion

Adsorption of Metal Salts onto Individual Beads in Well Plates. We first studied the adsorption of metal salts onto individual beads to optimize the conditions for synthesizing split−pool bead libraries in well plates. Our initial experiments involved adsorbing Pt from H_2PtCl_6 to determine metal distribution and uniformity on γ-alumina. We developed a one-sphere-at-a-time (OSAAT) approach for these experiments. Briefly, one alumina sphere was placed manually into each well of a 96 V-bottom well plate, and one or more adsorption/drying cycles were performed in that well. In a typical procedure to adsorb Pt onto each bead, beads were equilibrated in each well plate with 3 μL of solution at the concentration needed for the desired metal weight to be adsorbed onto each bead. Table 1 shows the results of ICP-AES analysis of three beads from each lot, indicating a good correlation between theoretical and measured compositions. The measurements were carried out at six different Pt

Table 2. Adsorption Sequences and Nominal Compositions of a Bead Library Made by the Row−Column Directed-Sorting Algorithm[a,b]

11111	44441	33441	22331	11331	44221	33221	22111
0005	4001	2201	0221	0203	2021	0221	0023
11111	44441	33441	22331	11331	44221	33221	22111
0005	4001	2201	0221	0203	2021	0221	0023
44411	33341	22341	11231	44231	33121	22121	11411
3002	1301	1121	0113	2111	0212	0032	1004
34411	23341	12341	41231	34231	23121	12121	41411
2102	1211	1112	1112	1211	0122	0023	2003
34411	23341	12341	41231	34231	23121	12121	41411
2102	1211	1112	1112	1211	0122	0023	2003
23311	12241	41241	34131	23131	12421	41421	34311
0212	1022	2012	1202	0212	1022	2012	1202
13311	42241	31241	24131	13131	42421	31421	24311
0203	2021	1112	1112	0203	2021	1112	1112
13311	42241	31241	24131	13131	42421	31421	24311
0203	2021	1112	1112	0203	2021	1112	1112
42211	31141	24141	13431	42431	31321	24321	13211
1022	1103	2012	1202	2111	0212	1121	0113
32211	21141	14141	43431	32431	21321	14321	43211
0122	1013	2003	2201	1211	0122	1112	1112
32211	21141	14141	43431	32431	21321	14321	43211
0122	1013	2003	2201	1211	0122	1112	1112
21111	14441	43441	32331	21331	14221	43221	32111
0014	3002	3101	0311	0212	1022	1121	0113

[a] The results shown are for one of four 96 well plates after four directed sorting cycles. Each well or bead is identified by a 5-digit adsorption sequence. For example, the first entry in row three (44411) signifies a bead history of three adsorptions of component 4 followed by two adsorptions of component 1. The four-digit composition below this sequence (3002) indicates that the bead contains three parts component 4 and two parts component 1. Note that the last adsorption step (the last digit in the 5-digit sequence) is the same for all beads in a given well plate. Note also that all compositions sum to 5, which is the number of adsorption steps in 4 split−pool cycles. [b] The algorithm generated all four components twice (0005, 0050, 0500, and 5000), 20 binaries with varied redundancy [0041, 0410, 1004, and 4100 (once); 0014, 1400, 0140 and 4001 (3 times); 3002 (6 times); 0032, 0320, 2003 and 3200 (5 times); 0023, 0230, 0203, 0302, 3020, 2030, and 2300 (6 times)], 24 ternaries with varied redundancy [0311, 3110, 1103, and 1031 (2 times); 1013, 0131, 1310, and 3101 (3 times); 0113, 1301, 3011, and 1130 (4 times); 1022 and 2210 (10 times); 0122, 2012, 1220, and 2201 (13 times); 0221 (11 times); 2102 (12 times); 0212, 1202, 2021, and 2120 (14 times)], and four quarternaries 27 times each (2111, 1211, 1112 and 1121). The missing binaries were 0104, 0401, 4010, and 1040.

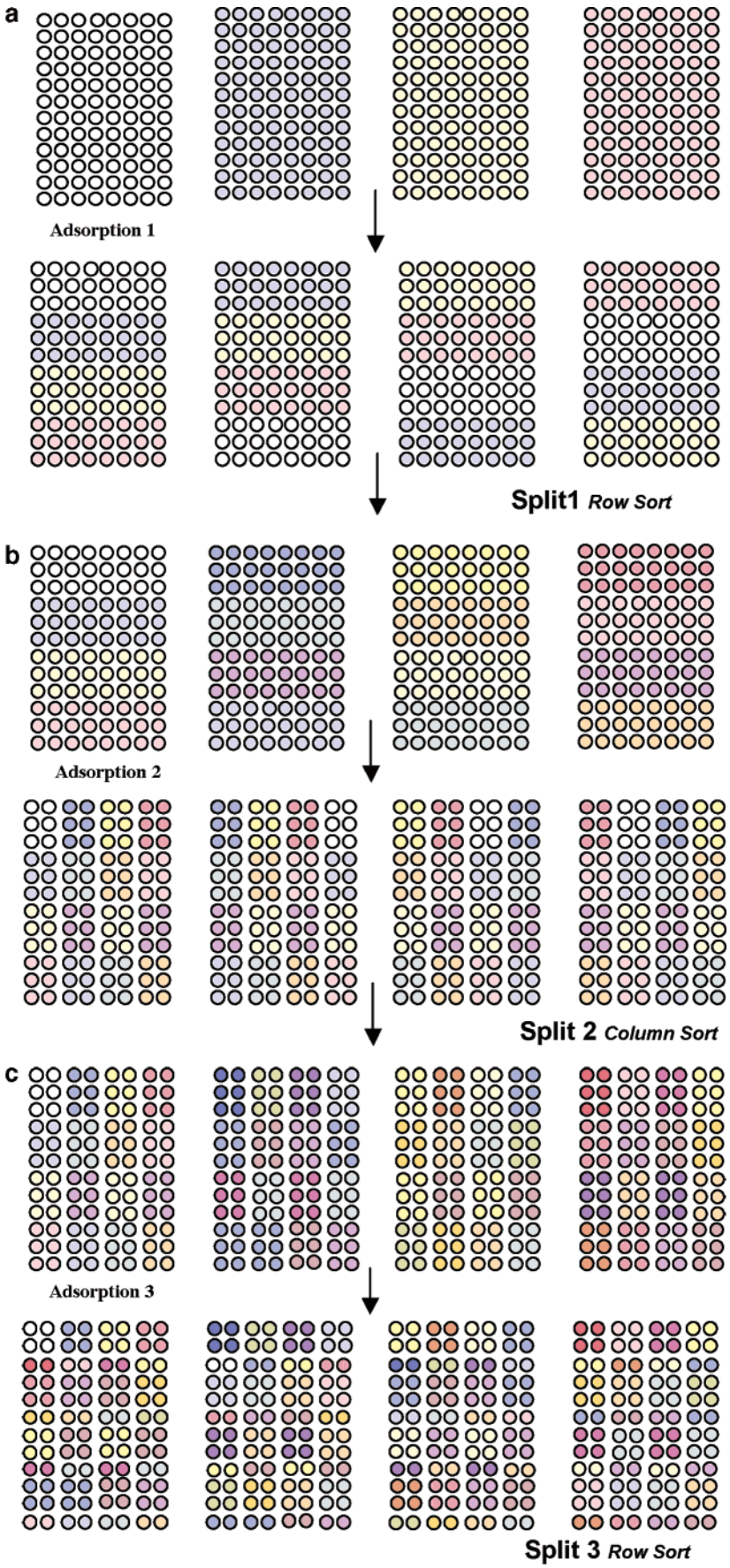

Figure 3. Color simulations of the directed-sorting process for a four-component, four-step, split−pool library: (a) first adsorption and one row transfer (first split); (b) second adsorption and first column transfer (second split); (c) third adsorption and second row transfer (third split).

Table 3. Summary Results of Simulations for Four-to-Eight-Component Bead Libraries Made in Standard 96-, 384-, and 1536-Well Plates Using the Row−Column Sorting Algorithm

components	steps	plate size	compositions	sequences	no. of wells
4	4	96	52	256	384
4	8	96	104	384	384
8	4	96	304	768	768
8	8	96	576	768	768
4	4	384	52	256	1536
4	8	384	148	1024	1536
8	4	384	520	2048	3072
8	8	384	1752	3072	3072
8	8	1536	1256	6144	12288

loadings. Analysis indicated that the beads were uniform in Pt impregnation (±4% variation from the average). We concluded that ICP-AES on Pt was not sensitive to variation in bead weight (7.1%) and bead diameter (7.7%) and possibly reflected variation in pipetting (3%) (See Supporting Information for variation in pipetting, bead diameter, and bead weight). Figure 4 shows EDS intensity as a function of position on cross-sectioned beads containing Pt. We also extended the OSAAT mode of adsorption to Ru, Ni, Au, Pd, Re, Ir, and Rh using 3 μL of metal salt solutions in 0.5 M HCl and obtained EDS elemental maps on cross-sectioned beads. We observed shadow artifacts in the EDS mapping, especially with the rhenium and iridium M lines. This artifact may arise from the low takeoff angle (30°) used for X-ray detection. The effect was less noticeable in the elemental L and M, lines which matched areas where the samples were flat. Under the conditions of EDS collection, the background due to the support (γ-alumina) was low. The bright spots on each image (Figure 4) were 3−4 μm in size (based on calibration of the IMIX software version used in the SEM). We therefore attribute all the bright spots to the presence of metal salts and found that they were evenly distributed. These experiments suggested that the OSAAT mode of adsorption could be adapted to the synthesis of split−pool libraries using the modified Vaccu-pettes as multipipettors and for suction during bead transfer.

Adsorption of Metal Salts under Incipient Wetness Conditions onto Beads in Well Plate Arrays. The essential difference between OSAAT and directed split−pool library synthesis was simply the movement of beads between adsorption steps. In our original split−pool experiments,[1] beads were loaded into 20-mL borosilicate glass vials and then adsorbed under impregnation (excess solvent) conditions. The beads were in close proximity to each other, and we postulated that eliminating this would greatly reduce heterogeneity and mixing problems. In OSAAT experiments, each bead sat in its own well and adsorbed solution under incipient wetness conditions. Our experiments under OSAAT conditions for adsorption of Pt, Ru, Ni, Au, Pd, Re, Ir, and Rh produced evenly distributed metal-loaded beads. The use of a well plate addresses the problem of metal ion transfer between pooled beads. All the beads (in individual wells) could be loaded with metal salt solutions in a single step, dried, and then transferred to the next set of well plates in directed-sorting operations that took the place of pooling and splitting. We thus optimized adsorption under OSAAT conditions and then applied the same conditions to directed combinatorial bead library synthesis.

Directed-Sorting Algorithm. Bead libraries were synthesized using a sorting algorithm conceptually similar to the randomization of colors in a Rubik's cube. One of the objectives in solving the Rubik's cube puzzle is to start from disjoint faces of the cube i.e., a mixture of colors, and end up with uniform color on each face of the cube. This is done by moving sections of the cube along row or column, similar to viewing each well plate as a matrix ($k \times l$) and shuffling rows and columns. Thus, the 3×3 Rubik's cube can be mapped onto a three-layer well-plate structure. The objective of our simulations and experiments, however, was the reverse: that is, start with uniform colors (first adsorption) and end up with a disjoint hypercube (the result of many adsorption steps and sequences in >3 compositional dimensions).

Conceptually, one can view each well plate as a bead positional matrix ($k \times l$) with a third variable j serving as the well-plate identifier. The number of components in a split−pool library (n) is fixed by the number of well-plates (indexed by j), analogous to the number of vials or reaction flasks in conventional split−pool synthesis, giving us the flexibility of choosing large or small split−pool libraries. We simulated the transfer sections of each well plate (i.e., beads along sets of rows or columns) to other well plates, with uniform metal salt adsorption in each well plate between sorting steps.

To rapidly simulate the sorting algorithms and assess the diversity of bead libraries they produced, a FORTRAN program (DIRECTSORT) was written, treating beads in wells (that replace vials) as members of a matrix (see Supporting Information). The program simulated different sorting algorithms and ran in a few seconds on a PC, allowing one to change the algorithm and see the results quickly. The first step in the process is adsorption of each component onto all the beads in each well plate. The program treats every adsorption step as unique in a given well plate and tracks this by adding the well plate index (j) to every bead (k,l) of a given well plate.

After the first adsorption there are rectangles of height (h) and width (w), where h is the total number of rows and w is the total number of columns in every well plate (See Figure 3a, top). The next step is to move members of a given row (k) in a well plate (j) to the same (j) or another ($j + 1$, $j + 2$, etc) plate. This implies that after the first adsorption and first row transfer there are rectangles of height (h/n) and width (w), in each well plate (Figure 3a, bottom). This row shuffle is followed by a second adsorption step, as shown in Figure 3b (top). At the end of the two adsorptions and one row transfer, each member of the matrix has two components (the first and second adsorption) and is deterministically identified. The next step is to move members of a given column (l) in a well plate to the same or to another well plate. This first column shuffle results in rectangles of height (h/n) and width (w/n), as shown in Figure 3b (bottom). The row/column shuffle alternates, with row shuffle after every odd adsorption step (counting the first as odd) and

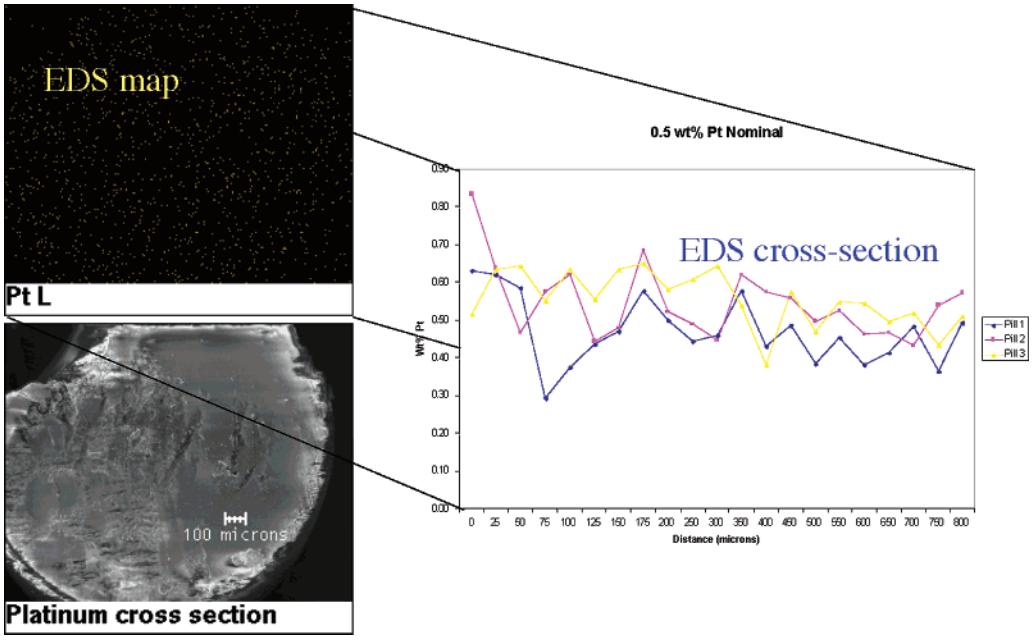

Figure 4. EDS mapping of composition for a 2-mg bead containing ~0.5% Pt. Each bright spot on the EDS map of the Pt L line varied between 3 and 4 μm.

column shuffle after every even adsorption step and proceeds to m steps, with total number of adsorptions being $m + 1$. The DIRECTSORT program counts the number of unique sequences of components and compositions (tallied as the total number of times a given component is present in the index of each element) and also gives a map of the final compositions.

Figure 3 illustrates the steps in a row/column shuffle using a four-component, 96-well plate (12 rows and 8 columns) library. The results of four split/pool steps (five adsorptions) are shown in Tables 2 and 3 for this library. This row/column shuffle algorithm, which also includes a shift of one row or column after each step to increase library diversity (see Experimental Section) captured 52 of the 56 possible compositions. We found that this algorithm missed four binaries (combinations of two of four elements) out of a possible 24, accounting for the difference (Table 2). Table 3 illustrates the number of unique compositions and sequences for libraries made with different well-plate sizes and numbers of split−pool steps.

We can see from Tables 2 and 3 that for small libraries (384 beads), there are as many unique sequences as there are wells (or beads) in the array, but there is some redundancy of compositions. The simulation procedure tracks individual beads as they are moved from a row/column of a given well plate to a row/column of another well plate. This process, thus, eliminates the need for physical tagging of beads. The number of physical manipulations (bead transfer and solution adsorption) for an n-component, m-step, directed-sorting library was $m(n^2 + 1) + 3n$, or on the order of mn^2 (See Supporting Information).

Synthesis and Analysis of Metal-Loaded Bead Libraries. For proof-of-concept, a four-component (Pt, Sn, Cu, and Ni), four-step (five adsorptions and four transfers), 96-well plate library was synthesized according to the row/column, directed-sorting algorithm. γ-Alumina beads used in these experiments were sorted by a commercial roller grader, and total metal content after four split pool cycles (five adsorption steps) was 0.25 wt % metal. The choice of metals and total loading was based on previous work on the methylcyclohexane (MCH) dehydrogenation reaction by Haensel et al. and Sinfelt et al.[19] Analysis of these bead libraries by μ-XRF and ICP-MS gave large relative errors because of the low loading of metal on the beads.

A second approach (column-only sort) was used to reduce the number of physical manipulations for reasonably diverse libraries and to provide at the same time eight copies of each bead for μ-XRF and ICP-MS analysis. For simplicity, four adsorptions of three metal salts was used. The column-only sort resulted in 3mn compositions and sequences prepared in 4mn steps. The total number of steps can be reduced by a factor of 2 by using suitably designed masks. This algorithm resulted in 36 compositions and used 48 physical manipulations for a library of 288 beads. The algorithm produced four sets of beads containing only one element; nine binary combinations (with two unique orders of addition each); and three ternary combinations, with one of three components twice (with five unique orders of addition each), as shown in Table 4. We separately synthesized all discrete binary and ternary combinations of elements at the resolution of four adsorption steps by manual pipetting. In the latter case, the total number of physical manipulations was 332, four times the number of pipetting steps as beads (82), and four plate transfers, as shown in Table 5.

To remove discrepancies due to interference from Sn and to check for analytical errors up to 1.0 wt %, we synthesized libraries of Pt, Cu, and Ni using ICP-MS standards of the three metals in a solution of 2.00% HCl (Hi-Purity Standards) by the column-shuffle algorithm. We postulated that using preanalyzed standards would help to reduce analytical errors. Two libraries were synthesized, one using the Vaccu-pette (Table 4) and another by manual pipetting (Table 5) using fresh well plates sealed in plastic prior to use.

Table 4. Adsorption Sequences Made by Column-Only Shuffle for a Three-Component, Three-Step Bead Library[a]

1111	2221	2211	3321	2111	3221	3211	1321	3111	1221	1211	2321
2222	3332	3322	1132	3222	1332	1322	2132	1222	2332	2322	3132
3333	1113	1133	2213	1333	2113	2133	3213	2333	3113	3133	1213

[a] Each row in the Table represents one of three 96-well plates after three directed-sorting cycles. The order of addition is represented by the same code as in Table 3. For example, the first entry in column two (2221) signifies a bead history of three adsorptions of component 2, followed by two adsorptions of component 1. The algorithm generated beads containing only one element (1111, 2222 and 3333), nine binary combinations with two unique orders of addition each (2221 and 1222; 2211 and 1221; 2111 and 1211; 3111 and 1113; 1133 and 3113; 1333 and 3133; 2333 and 3332; 3322 and 2332; 3222 and 2322) and three ternary combinations with one of three components twice and with five unique orders of addition each (1132, 1321, 1213, 3211, and 2113; 2213, 1322, 2132, 2321, and 3221; 3321, 1332, 3132, 2133, and 3213).

Table 5. Adsorption Sequences from Manual Pipetting in a Three-Component 96-Well Plate[a]

1111	1112	1112	1131	1122	1123	1121	1132	1133	1211	1212	1213
1231	1311	1312	1312	1221	1222	1223	1232	1322	1323	1333	1331
1332	1233	1321	2222	2223	2221	2232	2233	2231	2212	2213	2211
2322	2323	2321	2313	2122	2123	2121	2332	2333	2331	2133	2131
2111	2112	2113	2311	2313	2132	3333	3331	3332	3313	3332	3313
3311	3312	3323	3321	3322	3133	3131	3132	3123	3233	3231	3232
3113	3111	3112	3211	3212	3222	3223	3221	3122	3121	3213	0
0	0	0	0	0	0	0	0	0	0	0	0

[a] Each well or bead is identified by a four-digit adsorption sequence indicating the order of addition. For example, the first entry in column two (1112) signifies a bead history of three adsorptions of component 1, followed by one adsorption of component 2. Note that all compositions sum to 4, which is the number of adsorption steps in 3 split−pool cycles. 0 refers to no adsorption and was used to check for background.

The relative errors in μ-XRF, defined as the ratio of standard deviation to average of difference in theoretical amounts and measured μ-XRF values, were 39% in Pt, 35% in Ni, and 43% in Cu for theoretical metal content of 1.0 wt % on γ-alumina. We concluded that that μ-XRF was not a useful analytical tool for bead libraries of this type on the basis of relative errors due to bead diameter (7.7%), bead weight (7.1%), and pipetting (3%).

EPMA Analysis of Metal-Loaded Bead Libraries Made by the Row/Column Shuffle Algorithm. A few random samples were analyzed for Sn content using electron probe microanalysis (EPMA). Figure 5a and b show elemental profiles as a function of distance along each bead using EPMA, indicating that the metals are distributed throughout each bead with variation as a function of distance. We also observed that the signal from the EPMA saturated at 0.2 wt % metal.

ICP-MS Analysis of Metal-Loaded Beads Made by the Column-Only Shuffle Algorithm. The objective of these experiments was to test whether using the column shuffle algorithm adsorbed the desired quantities of metal on each bead, independent of variations in bead diameter, and weight. To compensate for matrix and order of addition effects, we synthesized mixed solutions of Cu, Co, and Ni from ICP-MS standards of the three metals in 10% HCl (Hi-Purity Standards) by the column-shuffle algorithm to give the compositions shown in Table 4. We then made a bead library by the same algorithm using 10 g of metal (from ICP-MS standards) per adsorption step and three sorting sequences, resulting in a total metal content of 1.7 wt % after four adsorptions. One library was synthesized using a Vaccu-pette in fresh well plates that were sealed in plastic prior to use. Pipetting had errors of 5% for all samples, and drifts in plasma resulted in errors of 6%. The instrumental measurement errors (confirmed using Cu and Ni spikes in preanalyzed standards) were 8% in samples containing Cu and Ni alone and 15% for both Cu and Ni in combinations of samples containing Cu and Ni and no Co. The instrumental measurement errors were 10% for samples containing Co alone, 22% for Cu, Ni, and Co (for samples having combinations of one or two additions of Ni or Cu or both, and one addition of Co) and 15% for Cu, Ni, and Co (for samples having two or three additions of Co and the other additions from combinations of Cu, Ni, or both). We postulated that Co formed cobalt phosphate and experimented with addition of spikes of Ni and Cu, ,that is adding more labile metals, but we were unsuccessful in reducing the magnitude of this analytical error. We also observed that the presence of Co led to larger analytical errors in the instrument.

We examined 22 of 36 compositions in Table 4: one sample each of four adsorptions of each element (1111, 2222, and 3333), one sample each of the 9 binary combinations (2221, 2211, 2111, 3111, 1133, 1333, 2333, 3322, 3222), and 14 samples from ternary combinations (1321, 3211, and 2113; 2213, 2132, 3221, and 2321; and 3321, 3132, and 3213). The 14 samples of ternary combinations also served to test order of addition trends in ICPMS analysis. We also examined nine duplicates (2221, 2111, 2213, 2132, 2321, 3121, 3111, 1333, and 1223) with and without Ni spikes. The results of predicted versus ICP-MS analytical results are part of Table 6. We observed that errors due to ICP-MS were distributed about two standard deviations around the mean for most of the samples. Although the ICP-MS analytical was not in absolute agreement with the theoretical amounts, these results confirm the sorting algorithm at the single-bead level using ICP-MS. ICP-MS was the only analytical technique we tried that was capable of characterizing individual beads at weight percents below the SEM detection limit (0.5 wt % for mixtures of metals).

Tests for Catalytic Activity Using LAMIMS. Laser-activated membrane introduction mass spectrometry (LAMIMS)[3] is a rapid screening technique based on membrane introduction mass spectrometry (MIMS) developed

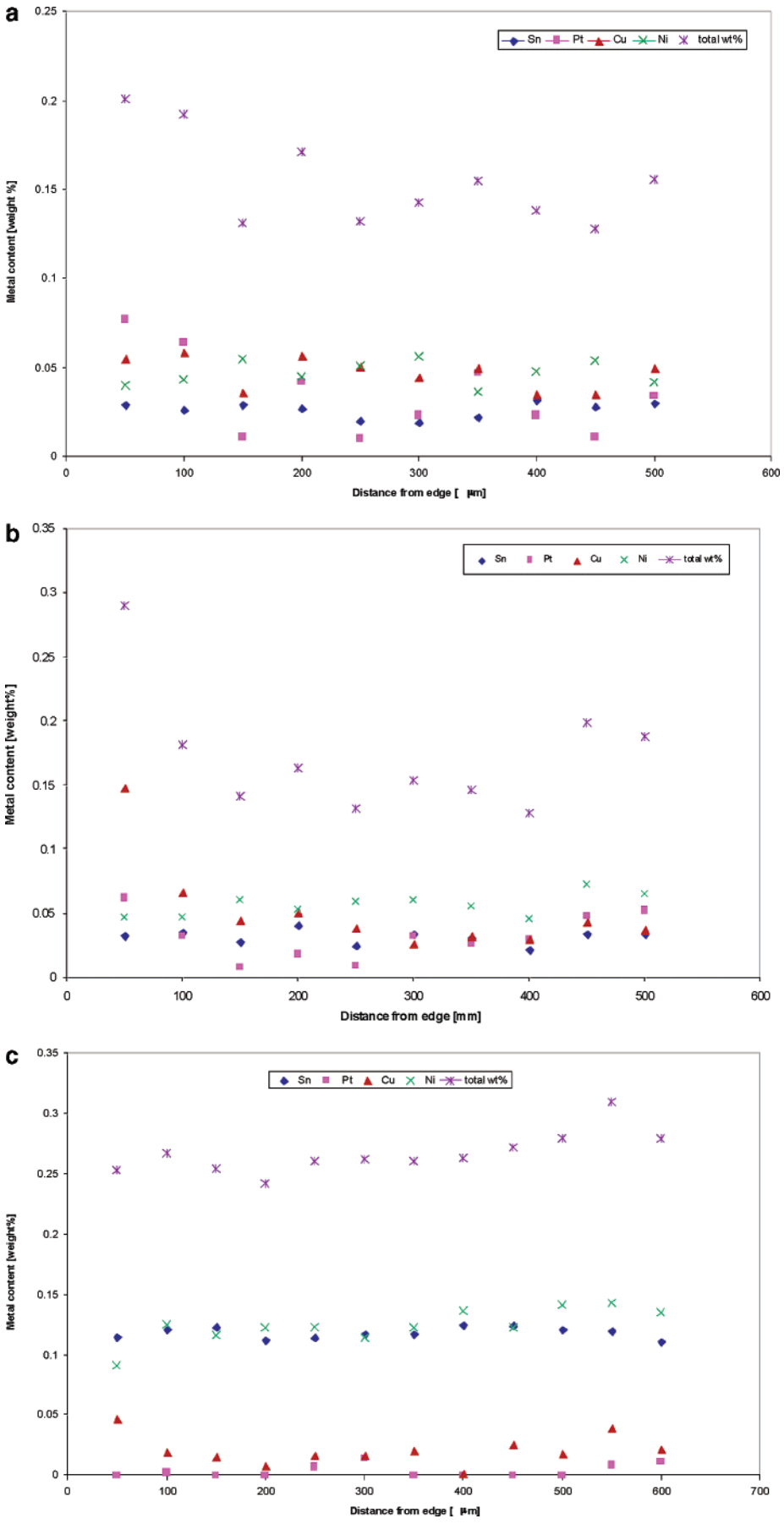

Figure 5. Electron probe microanalysis of metal-loaded beads as a function of position: (a) $Pt_{0.05}Ni_{0.05}Cu_{0.1}Sn_{0.05}$, (b) $Pt_{0.1}Ni_{0.05}Cu_{0.05}Sn_{0.05}$, and (c) $Ni_{0.15}Sn_{0.1}$. Subscripts indicate metal content in weight %.

Table 6. ICP-MS Analysis of 22 Bead Samples Made by Directed Sorting[a]

theor composition	anal. composition by ICPMS (× 4.0/1.7 wt %)	deviation from theoretical composition and instrumental standard deviation (in parentheses), both in percent		
		cobalt	nickel	copper
CoCoCoCo	$Co_{3.7}$	7.5 (10)		
NiNiNiNi	$Ni_{3.8}$		5 (8)	
CuCuCuCu	Cu_4			0 (8)
NiNiNiCo	$Co_1Ni_{2.9}$	0 (22)	3.3 (22)	
NiNiCoCo	$Co_{1.8}Ni_{1.8}$	10 (15)	10 (15)	
NiCoCoCo	$Co_{2.1}Ni_{0.9}$	30 (15)	10 (15)	
CuCoCoCo	$Co_{2.7}Cu_{0.9}$	10 (15)		10 (15)
CoCoCuCu	$Co_2Cu_{1.6}$	0 (15)		20 (15)
CoCuCuCu	$Co_{0.9}Cu_{2.6}$	10 (22)		13.3 (22)
NiCuCuCu	$Ni_{0.9}Cu_{2.3}$		10 (15)	23.3 (15)
CuCuNiNi	$Ni_{1.9}Cu_{1.7}$		5 (15)	15 (15)
CuNiNiNi	$Ni_{2.9}Cu_{0.9}$		3.3 (15)	10 (15)
CoCuNiCo	$Co_{1.4}Ni_{0.8}Cu_{0.3}$	30 (15)	20 (15)	70 (15)
CuNiCoCo	$Co_2Ni_1Cu_1$	0 (15)	0 (15)	0 (15)
NiCoCoCu	$Co_2Ni_1Cu_{0.95}$	0 (15)	0 (15)	5 (15)
NiNiCoCu	$Co_{0.8}$ $Ni_{0.9}Cu_{0.9}$	20 (22)	55 (22)	10 (22)
NiCoCuNi	$Co_{0.6}$ $Ni_{1.6}Cu_{0.9}$	40 (22)	20 (22)	10 (22)
NiCuNiCo	$Co_{0.6}Ni_{1.3}Cu_{0.95}$	40 (22)	35 (22)	5 (22)
CuNiNiCo	$Co_{0.8}Ni_{1.6}Cu_1$	20 (22)	20 (22)	0 (22)
CuCuNiCo	$Co_{0.8}Ni_1Cu_{1.9}$	20 (22)	0 (22)	5 (22)
CuCoCuNi	$Co_{0.7}Ni_{0.9}Cu_{1.6}$	30 (22)	10 (22)	20 (22)
CuNiCoCu	$Co_{0.6}$ $Ni_{0.9}Cu_{1.8}$	40 (22)	10 (22)	10 (22)

[a] The element code represents the four adsorption steps that resulted in a total of 1.7 wt % metal.

earlier by Cooks et al.[20] In LAMIMS, the catalyst bead array is separated from a mass spectrometer by a silicone membrane that maintains high vacuum on the spectrometer side but is sufficiently permeable to pass analytical quantities of reactant and product gases from the reactor side. The members of the bead array are heated serially to the reaction temperature by a laser. Because the reaction rate is strongly temperature-dependent, only the heated bead is catalytically active. Product gases detected by the mass spectrometer can thus be assigned to a particular bead, and the entire array can be screened by simply steering the laser beam from bead to bead.

We evaluated three well plates (a total of 288 beads) synthesized by the column-shuffle algorithm for catalytic activity using dehydrogenation of methylcyclohexane (MCH) as a probe reaction. The beads were evaluated in a LAMIMS reactor described in detail in ref 3. In a typical LAMIMS experiment, 96 metal-loaded beads were placed in the reactor. The metal-loaded beads were reduced under hydrogen by passing a 25-W laser at 25% of peak power over each bead for 6 min. The gas flow was switched to a mixture of methylcyclohexane (MCH) and hydrogen, the reduced beads were serially heated, and the mass spectrometer signal at $m/z = 91$ was detected as the toluene product signal.[3,21] At a mass-to-charge ratio of 91, the mass spectrometer detects the $[M - 1]^+$ fragment of toluene,[21] due to loss of a hydrogen atom to form the relatively stable benzyl cation. This cation is thought to undergo rearrangement to form the very stable tropylium cation, and the strong peak at $m/z = 91$ is a hallmark of compounds containing a benzyl unit.[21]

To quantify the mass spectrometer signal, a 1 wt % Pt on γ-alumina catalyst with a metal dispersion of 75%[3a] served as an internal standard in each run and was subjected to the same conditions (reduction and analysis for activity) as the bead samples made by directed sorting. The bead-to-bead variation in the toluene signal was determined for an array of 24 replicate 1 wt % Pt beads, which was subjected to five serial runs. The average signal varied by 2% over the five runs, and the relative standard deviation for individual measurements was 11%. We calculated an energy balance to verify that the laser sufficiently heated the samples during reduction and reaction (see Supporting Information).

We examined 8 replicates of 36 compositions including pure metals (Pt, Cu, and Ni with 1 wt % on γ-alumina), 9 binary combinations (with a redundancy of 2), and 3 unique ternary combinations (with a redundancy of 5 each). The LAMIMS area and peak height of the directed-sorting samples were normalized to the 1 wt % Pt on γ-alumina standard, described above.

We found that not all samples gave a detectable LAMIMS signal. The standard deviation in normalized LAMIMS analysis (area and peak height) was consistent between 0 and 0.1. To simplify the analysis, we chose to examine only compositions that had a detectable LAMIMS signal (reducing the number of examined compositions to 23). We also chose average LAMIMS peak height and an area of 0.2 as a lower bound based on the standard deviation in normalized LAMIMS peak height and area, reducing the number of compositions to 16. Seven of the 23 beads that had detectable LAMIMS signals had a LAMIMS peak height and area lower than 0.2 (usually on the order of 0.05) with a relative standard deviation of 50%. Table 7 shows the average, standard deviation, and relative standard deviation of LAMIMS peak height and area and μ-XRF analysis of these 16 selected samples.

We found that all eight replicate Pt on alumina samples synthesized by the column shuffle algorithm compared well to the 1 wt % Pt on γ-alumina standard. The relative errors in the normalized LAMIMS peak height and area were 9.6% and 11% respectively, indicating that the errors in the

Table 7. Average, Standard Deviation and Relative Standard Deviation in Normalized LAMIMS Area and μ-XRF of 16 Samples Synthesized by the Column-Shuffle Algorithm[a]

composition	av LAMIMS area relative to 1 wt % Pt	SD	rel SD (%)	av μ-XRF difference from theoretical (%)	SD in μ-XRF	rel SD in μ-XRF
NiNiPtPt (7)	0.23	0.1	43	36 (Pt)	10 (Pt)	29 (Pt)
				30 (Ni)	10 (Ni)	34 (Ni)
CuPtPtPt (8)	0.47	0.11	24	29 (Pt)	18 (Pt)	61 (Pt)
				32 (Cu)	15 (Cu)	47 (Cu)
PtPtPtCu (7)	0.23	0.05	21	19 (Pt)	12 (Pt)	61 (Pt)
				23 Cu)	9 (Cu)	37 (Cu)
PtPtPtPt (8)	1.17	0.11	10	29	11	39
CuCuCuNi (5)	0.31	0.06	19	32 (Ni)	12 (Ni)	38 (Ni)
				33 (Cu)	12 (Cu)	35 (Cu)
NiCuCuNi (4)	0.33	0.1	31	29 (Ni)	11 (Ni)	37 (Ni)
				27 (Cu)	14 (Cu)	51 (Cu)
CuCuNiNi (5)	0.27	0.08	29	27 (Ni)	9 (Ni)	33 (Ni)
				25 (Cu)	9 (Cu)	34 (Cu)
NiCuNiNi (4)	0.41	0.11	27	27 (Ni)	8 (Ni)	29 (Ni)
				30 (Cu)	7 (Cu)	24 (Cu)
CuNiNiNi (4)	0.22	0.07	32	29 (Ni)	12 (Ni)	43 (Ni)
				36 (Cu)	12 (Cu)	34 (Cu)
NiNiNiNi (4)	0.31	0.08	25	26	9	35
CuPtCuNi (4)	0.42	0.18	42	37 (Pt)	21 (Pt)	56 (Pt)
				31 (Ni)	14 (Ni)	44 (Ni)
				31 (Cu)	14 (Cu)	45 (Cu)
PtPtCuNi (4)	0.35	0.12	34	21 (Pt)	15 (Pt)	71 (Pt)
				32 (Ni)	13 (Ni)	42 (Ni)
				31 (Cu)	13 (Cu)	43 (Cu)
PtCuCuNi (4)	0.26	0.1	38	36 (Pt)	17 (Pt)	48 (Pt)
				33 (Ni)	15 (Ni)	45 (Ni)
				32 (Cu)	14 (Cu)	44 (Cu)
PtCuNiNi (7)	0.44	0.24	54	38 (Pt)	20 (Pt)	52 (Pt)
				28 (Ni)	14 (Ni)	50 (Ni)
				42 (Cu)	16 (Cu)	39 (Cu)
NiPtCuNi (4)	0.32	0.11	33	38 (Pt)	20 (Pt)	53 (Pt)
				37 (Ni)	14 (Ni)	37 (Ni)
				35 (Cu)	16 (Cu)	46 (Cu)
PtNiNiNi (4)	0.34	0.12	36	33 (Pt)	30 (Pt)	93 (Pt)
				35 (Ni)	12 (Ni)	33 (Ni)

[a] Numbers in parentheses in the first column denote number of samples (out of eight) included in the analysis. The remainder in each case had no detectable LAMIMS signal.

LAMIMS technique were lower than those of the μ-XRF analysis (39%) for Pt on γ-alumina. The LAMIMS technique using MCH dehydrogenation to toluene as a probe was sensitive to relative errors in bead weight (7.1%) and bead diameter (7.7%) and errors due to ICP-AES analysis of 1 wt % Pt from Table 2 (4%). We concluded earlier that errors in the ICP-AES analysis of 1 wt % Pt from Table 2 (4%) were mainly due to pipetting (3%). We estimated a molecule/site ratio of 657 on a one-bead basis, using theoretical Pt surface area of 276 m^2/g,[19] and concluded that sites were limiting under the conditions of the experiment.

We then examined the normalized LAMIMS peak area as a function of order of addition. Figure 6a−c shows the average normalized LAMIMS area as a function of Pt content and Pt as the last adsorption step (6a) and Ni content and last adsorption step (6b and c). The error bars in Figure 6a,c represent the standard deviation in average LAMIMS area. We found only one composition with Cu as the last adsorption step (PtPtPtCu) had average LAMIMS peak height and area greater than 0.2, and we included this composition as part of Figure 6a.

On the basis of average normalized LAMIMS area and relative standard deviation in normalized LAMIMS area and data from Table 7 and Figure 6a−c, we ranked the 16 selected samples for MCH dehydrogenation (assuming normalized LAMIMS area measured activity for MCH turnover) as PtPtPtPt > CuPtPtPt > (NiCuNiNi═CuPtCuNi═PtCuNiNi) > (PtPtCuNi═PtNiNiNi) > NiCuCuNi > (CuCuCuNi═NiNiNiNi═NiPtCuNi) > (CuCuNiNi = PtCuCuNi) > (PtPtPtCu = NiNiPtPt) > CuNiNiNi.

Overall, the most surprising trend was the variation in activity with order of addition for the same nominal composition in almost all samples that showed activity greater than 0.2. Figure 6a shows that the activity of Pt(0.75 wt %)/Cu(0.25 wt %) varied depending on the order of addition of Pt and Cu to the alumina beads. When Cu was adsorbed from ICP-MS standard solutions first, followed by three adsorptions of Pt, the average LAMIMS area was 47% that of pure Pt. When adsorption of copper followed three additions of Pt, the average LAMIMS area halved. We observed from Figure 6b that the activity of Ni(0.75 wt %)/Cu(0.25 wt %) also varied depending on the order of addition of Ni or Cu to the alumina beads. When the order of addition was Ni−Cu−Ni−Ni, the LAMIMS area was 44% that of pure Pt, but when the sequence was Cu−Ni−Ni−Ni, the average LAMIMS area halved. Order of addition trends were seen with a few combinations of Pt, Cu, and Ni consistently in a nonpredictive fashion, as shown in Figure 6c.

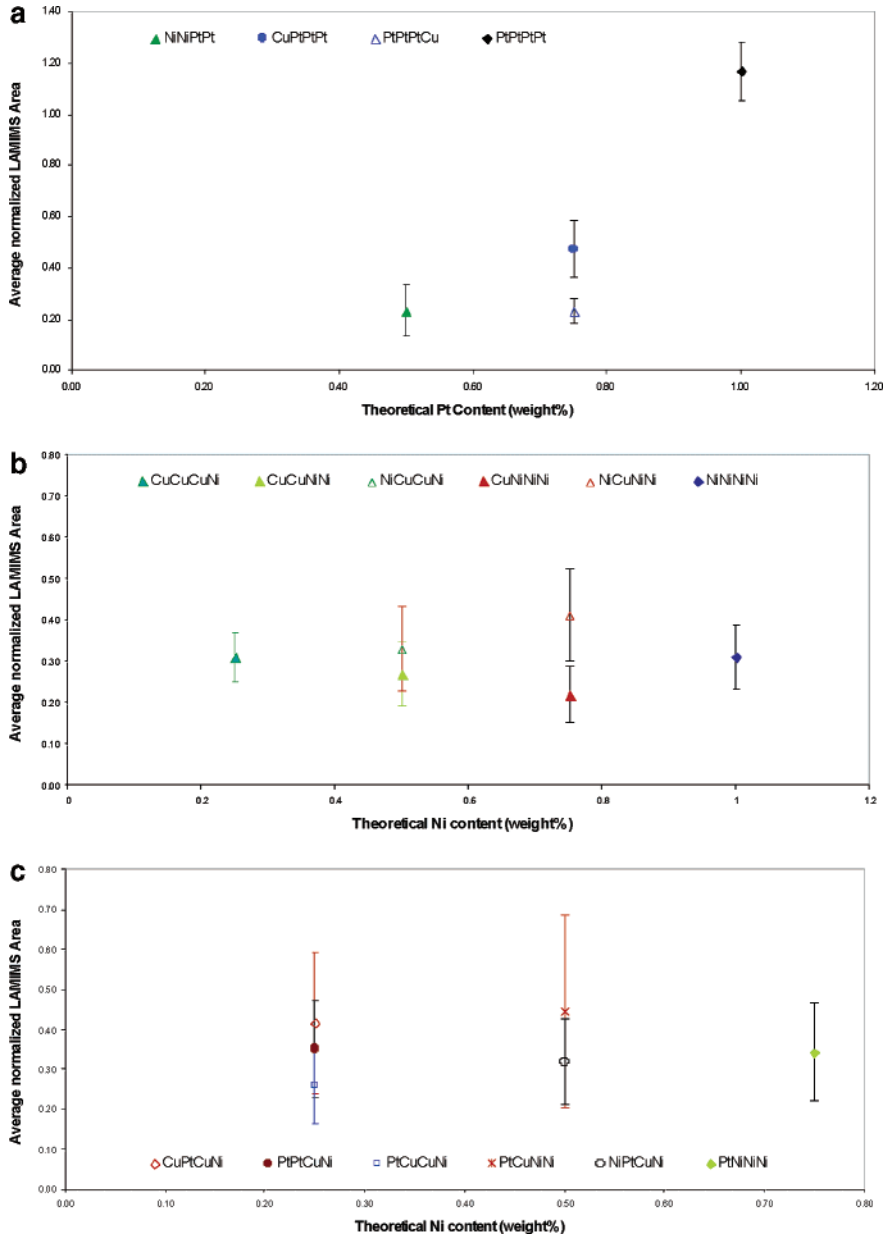

Figure 6. Average normalized LAMIMS area vs theoretical metal content (wt %), showing the effect of order of addition. Error bars represent one standard deviation. (a) Three samples with Pt as last adsorption and one with Cu as last adsorption: green closed triangles (NiNiNiNi), blue closed circles (CuPtPtPt), blue open triangles (PtPtPtCu), and black closed diamonds (PtPtPtPt). (b) Samples with Ni as last adsorption: blue closed triangles (CuCuCuNi), open green triangles (NiCuCuNi), green closed triangles (CuCuNiNi), open red triangles (NiCuNiNi), closed red triangles (CuNiNiNi), and blue closed diamonds (NiNiNiNi). (c) Samples with Ni as last adsorption: red open diamonds (CuPtCuNi), closed red circles (PtPtCuNi), open blue squares (PtCuCuNi), red asterisk (PtCuNiNi), open black circles (NiPtCuNi), green closed diamonds (PtNiNiNi).

The order of addition information could provide a very valuable tool in evaluating and optimizing catalysts of the same nominal composition. We believe that this could be the most powerful use of the current method. This study also evaluated catalytic activity as a function of precise amounts of energy (laser power) and should be useful in evaluating activity of catalyst, should availability of energy be an optimization parameter. As expected, in this model system, we were unsuccessful in finding a combination of elements on alumina that matched the activity of Pt for the MCH dehydrogenation reaction. The next step in combinatorial catalyst development would be to choose interesting compositions (based on average LAMIMS peak height and area comparable to a reference catalyst) and evaluate them in microreactors.

Using Direct Sorted LAMIMS Libraries in Catalyst Discovery. The experiments in this paper have quantified errors in synthesis and analysis of combinatorial libraries and the subsequent evaluation in a LAMIMS reactor. This study also showed that very little sample (2 mg) is required in analyzing catalytic activity of samples that showed minimal (~20% of that of Pt on alumina) to high conversion (equivalent to Pt on alumina at 100%) and, therefore, provides an alternative to screening using microreactors[22] for reactors that employ catalysts in the form of beads. Gembicki et al.[23] argue that catalysts and reactors have

evolved over the years to operate in a transient mode. The LAMIMS reactor inherently couples separation and reaction and can be adapted to run as a multifunctional transient reactor. Thus, it is possible that tools such as LAMIMS used in evaluation of combinatorial libraries will open up new applications and reactor designs.

Conclusions

The directed-sorting method is a simple benchtop route for preparing medium to large inorganic material bead libraries that do not require tagging or postsynthesis analysis. The main advantages of the method are its simplicity, ease of preparation, and low cost. In principle, the use of a multipipettor and corresponding analysis eliminates the need for robotic plotters that are often used in combinatorial chemistry, resulting in substantial cost savings. ICP-MS was the only analytical technique we used that was capable of analyzing mixtures of elements at loadings relevant to heterogeneous catalysis at the single bead level. The directed-sorting technique described in this paper also highlights the importance of order of addition in experiments seeking to optimize catalytic activity or other catalytic figures of merit. Difficulties with analytical techniques, bead weight, and diameter variation can by offset in part with the use of a chemical probe of bead activity, such as methylcyclohexane, using the LAMIMS reactor configuration.[3,24]

Acknowledgment. This work was performed with the support of the U.S. Department of Commerce, National Institute of Standards and Technology−Advanced Technology Program (Cooperative Agreement no. 70NANB9H3035) via subcontract with UOP LLC. R.R. thanks Prof. George Andrews for the references on Fisher and Yates; Anil Oroskar and Kurt Vandenbussche of UOP, John Sinfelt of Exxon-Mobil, Prof. Paul B. Weisz and Prof. Chunshan Song at The Pennsylvania State University for stimulating discussions; and John Kittleson and Mark Angelone at The Pennsylvania State University for performing the ICPMS and EPMA analyses.

Supporting Information Available. Experimental and analytical characterization details, synthetic details, Fortran program used to simulate the row/column shuffle algorithm, and energy balance calculations for LAMIMS experiments. This material is available free of charge via the Internet at http://pubs.acs.org.

References and Notes

(1) (a) Sun, Y.; Chan, B. C.; Ramnarayanan, R.; Leventry, W. M.; Bare, S. R.; Willis, R. R.; Mallouk, T. E. *J. Comb. Chem.* **2002**, *4*, 569. (b) The work reported in the current paper was presented at the Symposium on Chemistry of Petroleum and Emerging Technologies (paper PETR-004) at the 230th National Meeting of the American Chemical Society, Washington, DC, August 2005, and a brief preliminary account was accepted for publication in Preprints, American Chemical Society, Division of Petroleum Chemistry: **2005**, *50* (3), 278−281.

(2) (a) *Appl. Catal. A* **2003**, *254* (1), 1−170, focuses on applying combinatorial techniques to heterogeneous catalysis. (b) *Macromol. Rapid Commun.* **2004**, *25* (1), 1−386, focuses on applying tools and instruments used in combinatorial techniques and describes applications of the combinatorial technique to problems in polymers and other materials (semiconductors, catalysts). (c) *Meas. Sci. Technol.* **2005**, *16* (1), 1−316, is devoted to various aspects of combinatorial methods.

(3) (a) Nayar, A.; Kim, Y. T.; Rodriguez, J.; Willis, R. R.; Galloway, D. B.; Falaah, H. F.; Smotkin, E. S. *Appl. Surf. Sci.* **2004**, *223* (1−3), 118. (b) Nayar, A.; Liu, R.; Allen, R. J.; McCall, M. J.; Willis, R. R.; Smotkin, E. S. *Anal. Chem.* **2002**, *74*, 1933. (c) Nayar, A.; Liu, R.; Willis, R. R.; Smotkin, E. S. U.S. Patent Application, Publication, 2004/0077096, April 22, 2004. (d) Nayar, A.; Liu, R.; Willis, R. R.; Smotkin, E. S. U.S. Patent 6,923,939, August 2005.

(4) Mittasch, A. *Advances in Catalysis*; Academic Press, Inc.: New York, 1950; Vol. 2, pp 81−101.

(5) (a) Fisher R. A. *Statistical Methods, Experimental Design and Scientific Inference*; Oxford University Press: Oxford, 1990. (b) *Experimental Design*; selected papers of Frank Yates; Hafner Publishing Company: Connecticut, 1970.

(6) Hanak, J. J. *J. Mater. Sci.* **1970**, *5*, 964.

(7) (a) Xiang X.-D.; Sun, X.; Briceno, G.; Lou, Y.; Wang, K.-A.; Chang, H.; Wallace-Friedman, W. G.; Chen, S.; Schultz, P. G. *Science* **1995**, *268*, 1738. (b) Briceno, G.; Chang, H.; Sun, X.; Schultz, P. G.; Xiang, X.-D. *Science* **1995**, *270*, 273.

(8) (a) Moates, F. C.; Somani, M.; Annamalai, J.; Richardson, J. T.; Luss, D.; Willson, R. C. *IECR* **1996**, *35*, 4801. (b) Senkan, S. *Angew. Chem., Int. Ed.* **2001**, *40*, 312. (c) Jandeleit, B.; Schaefer, D. J.; Powers, T. S.; Turner, H. W.; Weinberg, W. H. *Angew. Chem., Int. Ed.* **1999**, *38*, 2494.

(9) (a) Reddington, E.; Sapienza, A.; Gurau, B.; Viswanathan, R.; Sarangapani, S.; Smotkin, E. S.; Mallouk, T. E. *Science* **1998**, *280*, 1735. (b) Chen, G.; Delafuente, D. A.; Sarangapani, S.; Mallouk, T. E. *Catal. Today* **2001**, *2443*, 1.

(10) (a) Danielson, E.; Golden, J. H.; McFarland, E. W.; Reaves, C. M.; Weinberg, W. H.; Wu, X. D. *Nature* **1997**, *389*, 944. (b) Danielson, E.; Devenney, M.; Giaquinta, D. M.; Golden, J. H.; Haushalter, R. C.; McFarland, E. W.; Poojary, D. M.; Reaves, C. M.; Weinberg, W. H.; Wu, X. D. *Science* **1998**, *279*, 837.

(11) Van Dover, R. B.; Schneemeyer, L. F.; Fleming, R. M. *Nature* **1998**, *392*, 162.

(12) (a) Lebl, M. *J. Comb. Chem.* **1999**, *1*, 3. (b) Lam, K. S.; Lebl, M.; Krchňák, V. *Chem. Rev.* **1997**, *97*, 411.

(13) (a) Lam, K. S.; Salmon, S. E.; Hersh, E. M.; Hruby, V. J.; Kazmierski, W. M.; Knapp, R. J. *Nature* **1991**, *354*, 82. (b) Houghten, R. A.; Pinilla, C.; Blondelle, S. E.; Appel, J. R.; Dooley, C. T.; Cuervo, J. H. *Nature* **1991**, *354*, 84. (c) Kozmin, S. A.; Wang, Y. *Angew. Chem., Intl. Ed.* **2003**, *42*, 903.

(14) Miller, C. T.; Mann, G.; Havrilla, G. J.; Wells, C. A.; Warner, B. P.; Baker, R. T. *J. Comb. Chem.* **2003**, *5*, 245.

(15) Klein, J.; Zech, T.; Newsam J. M.; Schunk, S. A. *Appl. Catal. A* **2003**, *254* (1), 121.

(16) *Experimental Design for Combinatorial and High Throughput Materials Development*; Cawse J. N., Ed.; John Wiley and Sons: NJ, 2003.

(17) *Combinatorial Chemistry: A Practical Approach*; Fenniri, H., Ed.; Oxford University Press: Oxford, UK, 2000.

(18) (a) Mitsche, R. T. U.S. Patent 3943070 19760309, 1976. (b) Steenberg, L. R.; Vesely, K. D. Ger. Offen. Patent DE 2048434 19720406, 1972.

(19) (a) Haensel, V.; Donaldson, G. R. *IECR* **1951**, *43*, 2102. (b) Sinfelt, J. H.; Hurwitz, H.; Schulman, R. A. *J. Phys. Chem.* **1960**, *64*, 1559. (c) Sinfelt, J. H. *J. Mol. Catal. A: Chem.* **2000**, *163*, 123 2000. (d) Reyes, S. C.; Sinfelt, J. H.; DeMartin, G. J. *J. Phys. Chem B* **2005**, *109*, 2421.

(20) (a) Kotiaho, T.; Lauritsen, F. R.; Choudhari, T. K.; Cooks, R. G.; Tsao, G. T. *Anal. Chem.* **1991**, *63*, 875A. (b) Kotiaho, T.; Lauritsen, F. R.; Choudhari, T. K.; Cooks, R. G.; Tsao, G. T. *Anal. Chem.* **1991**, *63*, 882A.

(21) NIST Mass Spectra Data Center; Mass Spectra. In *NIST Chemistry WebBook*; NIST Standard Reference Database Number 69; Linstrom, P. J., Mallard, W. G., Eds.; June 2005, National Institute of Standards and Technology: Gaithersburg, MD, 20899. http://webbook.nist.gov (accessed June 10, 2005).

(22) Baertsch, C. D.; Schmidt, M. A.; Jensen K. F. *Chem. Commun.* **2004**, *22*, 2610.

(23) Gembicki, S. A.; Vanden Bussche, K. M.; Oroskar, R. A. *Chem. Eng. Sci.* **2003**, *58*, 549.

(24) (a) Swenson, L. R.; Brandvold, T. A.; McCall, M. J.; Willis, R. R. U.S. Patent 6,844,198, January 2005. (b) Swenson, L. R.; Brandvold, T. A.; McCall, M. J.; Willis, R. R. PCT Int. Appl. WO 2002088674, 2002. (c) Swenson, L. R.; Brandvold, T. A.; McCall, M. J.; Vanden Bussche, K. M.; Willis, R. R. U.S. Patent 6,808,928, October 2004. (d) Swenson, L. R.; Brandvold, T. A.; McCall, M. J.; Vanden Bussche, K. M.; Willis, R. R. PCT Int. Appl. WO 2002088675, 2002.

CC050137R